Wavefront reconstruction for XAO

Iuliia Shatokhina, Mariya Zhariy, Ronny Ramlau
Industrial Mathematics Institute,
Johannes Kepler University, Linz, Austria
e-mail: iuliia.shatokhina@indmath.uni-linz.ac.at

1. Introduction

We present our work done within the Austrian InKind project 'Mathematical algorithms and software for E-ELT Adaptive Optics'. In particular, we are concerned with eXtreme Adaptive Optics (XAO). Our aim is the development of fast algorithms for reconstructing the incoming wavefront ϕ from the sensor measurements $\boldsymbol{s}$. Possible choices of sensors for the XAO system are Pyramid WFS (P-WFS) and Roof WFS (R-WFS). Among other parameters of the considered XAO system are: telescope diameter $\mathbf{42}\boldsymbol{m}$, $\mathbf{200} \times \mathbf{200}$ WFS subapertures, integration time of $\mathbf{0.3}\boldsymbol{ms}$ $(\sim \mathbf{3}\boldsymbol{KHz})$.

2. Non-modulated Pyramid WFS

Under the closed loop assumption of small wavefront perturbations, $|\phi| << \mathbf{1}$ rad, we linearize [4,7] the transmission mask P-WFS model from [2] as

$$\boldsymbol{S_x} = -\boldsymbol{PH_x(P\phi)} + \boldsymbol{P\phi H_x(P)} - \boldsymbol{H_{xy}(P)H_y(P\phi)} + \boldsymbol{H_{xy}(P\phi)H_y(P)}, \quad (1)$$

$$\boldsymbol{S_y} = -\boldsymbol{PH_y(P\phi)} + \boldsymbol{P\phi H_y(P)} - \boldsymbol{H_{xy}(P)H_x(P\phi)} + \boldsymbol{H_{xy}(P\phi)H_x(P)}. \quad (2)$$

Here $\boldsymbol{P}$ denotes the telescope aperture mask, the transforms $\boldsymbol{H_x}, \boldsymbol{H_y}$ and $\boldsymbol{H_{xy}}$ are defined for a function $\boldsymbol{f} : \mathbb{R}^2 \to \mathbb{C}$ as

$$(\boldsymbol{H_x f})(\cdot, \boldsymbol{y}) := (\boldsymbol{Hf}(\cdot, \boldsymbol{y})), \quad (\boldsymbol{H_y f})(\boldsymbol{x}, \cdot) := (\boldsymbol{Hf}(\boldsymbol{x}, \cdot)), \quad (\boldsymbol{H_{xy} f}) := \boldsymbol{H_x}(\boldsymbol{H_y f}),$$

where $\boldsymbol{H}$ is the Hilbert transform (HT) defined as

$$(\boldsymbol{Hf})(\boldsymbol{x}) := \frac{\mathbf{1}}{\pi}\boldsymbol{p.v.} \int_{\mathbb{R}} \frac{\boldsymbol{f(t)}}{\boldsymbol{x - t}}\boldsymbol{dt}. \quad (3)$$

If $\boldsymbol{P} = \mathbf{1}$ (infinite telescope size assumption), the model (1)-(2) simplifies to [4]

$$\boldsymbol{S_x} = -\boldsymbol{H_x}\phi, \qquad \boldsymbol{S_y} = -\boldsymbol{H_y}\phi. \quad (4)$$

Hilbert Transform with Mean Restoration (HTMR)

Consider the simple model (4). Assumption: $\int_\Omega \phi(\boldsymbol{x}, \boldsymbol{y})\boldsymbol{dxdy} = \mathbf{0}$.
Task: reconstruct the phase ϕ such that its mean value equals zero.
Inverse: The inverse Hilbert transform is given by $\boldsymbol{H^{-1}} = -\boldsymbol{H}$.
Reconstruction: $\boldsymbol{f} = -\boldsymbol{H}(\boldsymbol{Hf})$.
Mean: In practice, the mean value $\bar{\boldsymbol{f}}$ is lost, $\boldsymbol{f^{rec}} = -\boldsymbol{H}(\boldsymbol{Hf}) = \boldsymbol{f} - \bar{\boldsymbol{f}}$.

HTMR Algorithm

1. Apply the HT rowwise to $\boldsymbol{S_x}$ and columnwise to $\boldsymbol{S_y}$,

$$\phi_{\boldsymbol{x}}^{\boldsymbol{rec}}(\boldsymbol{x}, \cdot) = \boldsymbol{H_x S_x} = \boldsymbol{H_x}(-\boldsymbol{H_x}\phi) = \phi(\boldsymbol{x}, \cdot) - \overline{\phi(\boldsymbol{x}, \cdot)}, \quad (5)$$

$$\phi_{\boldsymbol{y}}^{\boldsymbol{rec}}(\cdot, \boldsymbol{y}) = \boldsymbol{H_y S_y} = \boldsymbol{H_y}(-\boldsymbol{H_y}\phi) = \phi(\cdot, \boldsymbol{y}) - \overline{\phi(\cdot, \boldsymbol{y})}. \quad (6)$$

2. Restore the mean values (as in CuRe [6]),

$$\phi = \phi_{\boldsymbol{x}}^{\boldsymbol{rec}} + \frac{\mathbf{1}}{\boldsymbol{D}}\int_{\mathbf{0}}^{\boldsymbol{D}} \phi_{\boldsymbol{y}}^{\boldsymbol{rec}}(\boldsymbol{x}, \cdot)\boldsymbol{dx}, \qquad \phi = \phi_{\boldsymbol{y}}^{\boldsymbol{rec}} + \frac{\mathbf{1}}{\boldsymbol{D}}\int_{\mathbf{0}}^{\boldsymbol{D}} \phi_{\boldsymbol{x}}^{\boldsymbol{rec}}(\cdot, \boldsymbol{y})\boldsymbol{dy}. \quad (7)$$

Speed analysis: In case of sequential implementation, computational effort is of the same order as for the 2D Fourier transform, $\sim \boldsymbol{N^2 \log(N)}$, where $\boldsymbol{N}$ is the number of subapertures in 1D. In case of parallel implementation, computational effort is of the same order as for the 1D Fourier transform, $\sim \boldsymbol{N \log(N)}$.
Error sources: incomplete data due to the circular aperture mask; data sampling (subaperture discretization); aliasing due to the finite Fourier transform.
Mean restoration: over the square; over the circular aperture (see details in [7]).

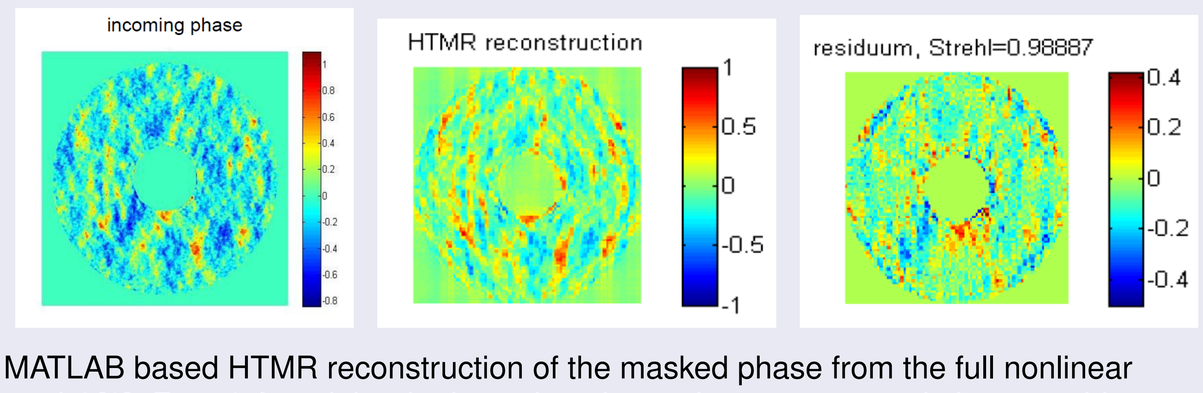

MATLAB based HTMR reconstruction of the masked phase from the full nonlinear model [2]. From left to right: the incoming phase, the reconstructed phase, residuum and Strehl ratio. Mean restoration is done over the square. Sampling over the subapertures is not considered.

HTMR + Fixed-Point Iteration (FPI)

Consider the full linearized model (1)-(2). Set $\boldsymbol{R_x}, \boldsymbol{R_y}$ as

$$\boldsymbol{R_x} = \boldsymbol{P\phi H_x(P)} - \boldsymbol{H_{xy}(P)H_y(P\phi)} + \boldsymbol{H_{xy}(P\phi)H_y(P)}, \quad (8)$$

$$\boldsymbol{R_y} = \boldsymbol{P\phi H_y(P)} - \boldsymbol{H_{xy}(P)H_x(P\phi)} + \boldsymbol{H_{xy}(P\phi)H_x(P)}. \quad (9)$$

Then (1)-(2) reads as

$$\boldsymbol{S_x} - \boldsymbol{R_x}(\phi) = -\boldsymbol{PH_x(P\phi)}, \qquad \boldsymbol{S_y} - \boldsymbol{R_y}(\phi) = -\boldsymbol{PH_y(P\phi)}. \quad (10)$$

Based on this 'new' data, and the HTMR reconstruction from the masked Hilbert data,
1. Set $\phi_{\mathbf{0}} = \mathbf{0}$, $\bar{\phi}_{\mathbf{0}} = \mathbf{0}$.
2. For each $\boldsymbol{n} \geq \mathbf{1}$ find $\bar{\phi}_{\boldsymbol{n}}$ solving (approximately)

$$\boldsymbol{S_x} - \boldsymbol{R_x}(\phi_{\boldsymbol{n-1}}) = -\boldsymbol{PH_x(P\phi_n)}, \qquad \boldsymbol{S_y} - \boldsymbol{R_y}(\phi_{\boldsymbol{n-1}}) = -\boldsymbol{PH_y(P\phi_n)} \quad (11)$$

via the HTMR algorithm,

$$\bar{\phi}_{\boldsymbol{n}} = \boldsymbol{HTMR}(\boldsymbol{S_x} - \boldsymbol{R_x}(\phi_{\boldsymbol{n-1}}), \boldsymbol{S_y} - \boldsymbol{R_y}(\phi_{\boldsymbol{n-1}})). \quad (12)$$

3. Set $\phi_{\boldsymbol{n}} = \frac{\mathbf{1}}{\mathbf{2}}(\phi_{\boldsymbol{n-1}} + \bar{\phi}_{\boldsymbol{n}})$.

HTMR + FPI (cont.)

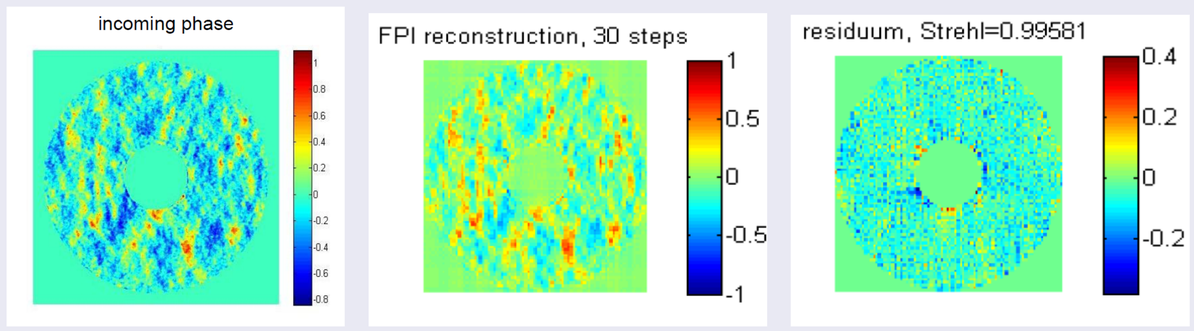

Reconstruction from the full nonlinear model [2] via FPI with 30 steps, the mean restoration is done over the square. From left to right: the incoming phase, the reconstructed phase, the residual. Sampling over the subapertures is not considered.

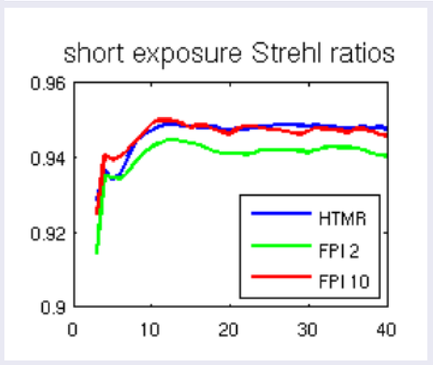

Closed loop comparison of two methods

Closed loop SE Strehl ratios reached with the reconstruction methods: HTMR, FPI with 2 iterations per loop, and FPI with 10 iterations per loop. Circular aperture mask with central obstruction and the subaperture discretisation included.

3. Modulated Roof WFS

Under the closed loop assumption, the modulated Roof WFS transmission mask model [1,3] reads as

$$\boldsymbol{S_x}(\boldsymbol{x}, \boldsymbol{y}) = (\boldsymbol{R}\phi)(\boldsymbol{x}, \boldsymbol{y}) = \frac{\mathbf{1}}{\mathbf{2}\pi}\int_{-\boldsymbol{X}(\boldsymbol{y})}^{\boldsymbol{X}(\boldsymbol{y})} \frac{[\phi(\boldsymbol{x'}, \boldsymbol{y}) - \phi(\boldsymbol{x}, \boldsymbol{y})]\boldsymbol{J_0}[\alpha_\lambda(\boldsymbol{x'} - \boldsymbol{x})]}{\boldsymbol{x} - \boldsymbol{x'}}\boldsymbol{dx'}, \quad (13)$$

where $\boldsymbol{J_0}$ denotes the zero-order Bessel function of the first kind; α_λ is the modulation parameter, defined via the modulation radius α by $\alpha_\lambda = \frac{2\pi\alpha}{\lambda}$, $\alpha = \frac{r\lambda}{D}$, $\boldsymbol{r} \in \mathbb{N}$; $-\boldsymbol{X}(\boldsymbol{y}), \boldsymbol{X}(\boldsymbol{y})$ denote the telescope aperture boundaries.

Taylor series approximation

We suggest a fast numerical implementation [5] of the model (13), based on the Taylor series expansion of the Bessel function $\boldsymbol{J_0}$,

$$\boldsymbol{S_x}(\boldsymbol{x}, \boldsymbol{y}) \approx (\boldsymbol{Q}\phi)(\boldsymbol{x}, \boldsymbol{y}) - \phi(\boldsymbol{x}, \boldsymbol{y}) \cdot \boldsymbol{h}(\boldsymbol{x}) - (\boldsymbol{T}\phi)(\boldsymbol{x}, \boldsymbol{y}) + \phi(\boldsymbol{x}, \boldsymbol{y}) \cdot (\boldsymbol{T}(\mathbf{1}))(\boldsymbol{x}, \boldsymbol{y}), \quad (14)$$

$$(\boldsymbol{Q}\phi)(\boldsymbol{x}, \boldsymbol{y}) \approx \sum_{\boldsymbol{m}=1}^{\bar{\boldsymbol{M}}} \frac{\boldsymbol{c'(m)}}{\mathbf{2}\pi} \int_{-\boldsymbol{X}(\boldsymbol{y})}^{\boldsymbol{X}(\boldsymbol{y})} \phi(\boldsymbol{x'}, \boldsymbol{y})(\boldsymbol{x'} - \boldsymbol{x})^{\mathbf{2}\boldsymbol{m}-\mathbf{1}}\boldsymbol{dx'},$$

$$\boldsymbol{h}(\boldsymbol{x}) \approx \sum_{\boldsymbol{m}=1}^{\bar{\boldsymbol{M}}} \frac{\boldsymbol{c'(m)}}{\mathbf{4}\pi\boldsymbol{m}} \left((\boldsymbol{X}(\boldsymbol{y}) - \boldsymbol{x})^{\mathbf{2}\boldsymbol{m}} - (-\boldsymbol{X}(\boldsymbol{y}) - \boldsymbol{x})^{\mathbf{2}\boldsymbol{m}}\right),$$

where the coefficients $\boldsymbol{c'(m)}$ are given by $\boldsymbol{c'(m)} = \frac{(-\mathbf{1})^{\boldsymbol{m}+\mathbf{1}}}{(\boldsymbol{m}!)^2}\left(\frac{\mathbf{1}}{\mathbf{4}}\alpha_\lambda^2\right)^{\boldsymbol{m}}$. Here $\boldsymbol{T}$ denotes the finite Hilbert transform,

$$(\boldsymbol{Tf})(\boldsymbol{x}, \cdot) := \frac{\mathbf{1}}{\pi}\boldsymbol{p.v.}\int_{-\boldsymbol{X}(\boldsymbol{y})}^{\boldsymbol{X}(\boldsymbol{y})} \frac{\boldsymbol{f(t, \cdot)}}{\boldsymbol{x - t}}\boldsymbol{dt}. \quad (15)$$

The model (14) reduces to

$$\boldsymbol{S_x} \approx \tilde{\boldsymbol{Q}}\phi - \phi \cdot \tilde{\boldsymbol{h}}, \quad (16)$$

where $\tilde{\boldsymbol{Q}} = \boldsymbol{Q} - \boldsymbol{T}$, and $\tilde{\boldsymbol{h}} = \boldsymbol{h} - \boldsymbol{T}(\mathbf{1})$.

Fixed-Point Iteration (FPI)

We consider a modified fixed-point iterative method for solving (16),

$$\phi_{\boldsymbol{k+1}} = \frac{(\tilde{\boldsymbol{Q}}\phi_{\boldsymbol{k}} - \boldsymbol{S_x})\tilde{\boldsymbol{h}} + \alpha\phi_{\boldsymbol{k}}}{\tilde{\boldsymbol{h}}^2 + \alpha}. \quad (17)$$

Theoretically, the iterates converge to the solution, provided that α is big enough, and $|\alpha| > ||\tilde{\boldsymbol{Q}}||$. Numerical study of the suggested algorithm is an on-going work.

Conjugate Gradient on the Normal Equation (CGNE)

For solving (16) we consider another iterative method, CGNE, i.e., we apply the CG algorithm to the normal equation $\boldsymbol{R^*R}\phi = \boldsymbol{R^*S_x}$. For the modulated Roof WFS operator $\boldsymbol{R}$, its adjoint $\boldsymbol{R^*}$ is given by $\boldsymbol{R^*} = -\boldsymbol{R}$. Therefore, both operators can be evaluated fast. Numerical study of the suggested algorithm is an on-going work.

References

1. A. Burvall, E. Daly, S.R. Chamot, Ch. Dainty. Linearity of the pyramid wavefront sensor. Optics Express, 14 (25): 11925–11934, 2006.
2. V. Korkiakoski, Ch. Vérinaud, M. Le Louarn, R. Conan. Comparison between a model-based and a conventional pyramid sensor reconstructor. Applied Optics, 46(24): 6176–6184, 2007.
3. Ch. Vérinaud. On the nature of the measurements provided by a pyramid wave-front sensor. Optics Communications, 233: 27–38, 2004.
4. Iu. Shatokhina. Simulation of the non-modulated pyramid wavefront sensor. Technical Report E-TRE-AAO-528-0007, Austrian In-Kind Contribution - AO, 2011.
5. Iu. Shatokhina. Simulation of the modulated pyramid and roof wavefront sensors. Technical Report E-TRE-AAO-528-0011, Austrian In-Kind Contribution - AO, 2011.
6. M. Zhariy, A. Neubauer, M. Rosensteiner, R. Ramlau. Cumulative wavefront reconstructor for the Shack-Hartmann sensor. Inverse Problems and Imaging, accepted, 2011.
7. M. Zhariy. Hilbert transform reconstructor for non-modulated PWS measurements. Technical Report E-TRE-AAO-528-0013, Austrian In-Kind Contribution - AO, 2011.